

55 Cancri: A Laboratory for Testing Numerous Conjectures about Planet Formation

Dimitris M. Christodoulou^{1,2} and Demosthenes Kazanas³

ABSTRACT

Five planets are presently believed to orbit the primary star of 55 Cnc, but there exists a large 5 AU gap in their distribution between the two outermost planets. This gap has attracted considerable interest because it may contain one or more lower-mass planets whose existence is not contradicted by long-term orbit stability analyses, in fact it is expected according to the "packed planetary systems" hypothesis and an empirical Titius-Bode relation recently proposed for 55 Cnc. Furthermore, the second largest planet is just the second farthest and it orbits very close to the star. Its orbit, the most circular of all, appears to be nearly but not quite commensurable with the orbit of the third planet, casting doubt that any migration or resonant capture of the inner planets has ever occurred and lending support to the idea of "in-situ" giant planet formation by the process of core accretion. All of the above ideas will be tested in the coming years in this natural laboratory as more observations will become available. This opportunity presents itself in conjunction with a physical model that relates the orbits of the observed planets to the structure of the original protoplanetary disk that harbored their formation at the early stages of protostellar collapse. Using only the 5 observed planets of 55 Cnc, this model predicts that the surface density profile of its protoplanetary disk varied with distance R precisely as $\Sigma(R) \propto R^{-3/2}$, as was also found for the minimum-mass solar nebula. Despite this similarity, the disk of 55 Cnc was smaller, heavier, and less rotationally supported than the solar nebula, so this system represents a different mode of multi-planet formation compared to our own solar system.

Subject headings: planets and satellites: formation—planetary systems: formation—planetary systems: protoplanetary disks—stars: individual (HD 75732, ρ^1 Cancri, 55 Cancri)—stars: individual (HD 160691, μ Ara, GJ 691)

¹Math Methods, 54 Middlesex Tpke, Bedford, MA 01730. E-mail: dimitris@mathmethods.com

²University of Massachusetts Lowell, Dept. of Mathematical Sciences, Olney Hall, Room 428, Lowell, MA 01854. E-mail: Dimitris_Christodoulou@uml.edu

³NASA/GSFC, Code 663, Greenbelt, MD 20771. E-mail: Demos.Kazanas@nasa.gov

1. Introduction

1.1. Observations

Eighteen years of Doppler–shift measurements of the primary star in the nearby binary system 55 Cancri (HD 75732; hereafter 55 Cnc) have gradually raised the number of orbiting planets from 1 (Butler et al. 1997), to 3 (Marcy et al. 2002), to 4 (McArthur et al. 2004), and recently to 5 (Fischer et al. 2008). Although the 4 inner planets are closely packed together (their semimajor axes $a < 1$ AU), the orbits of all 5 planets are remarkably circular (see Table 1) and presumably coplanar. The system exhibits astonishing regularity, reminiscent only of the planetary order in our solar system and unmatched by any other currently known multiple–planet extrasolar system (for reviews of orbital and dynamical characteristics of exoplanets, see Marcy et al. [2005] and Butler et al. [2006]). The most massive planet, 55 Cnc d with $a = 5.77$ AU and a minimum mass¹ of 3.835 Jupiter masses (Table 1), is the most distant gaseous giant known among exoplanets with well–defined orbits and, like Jupiter, it orbits beyond 5 AU from the star. Furthermore, there are no giant planets in the area roughly between 1 and 5 AU, just like in our solar system. In fact, no planets have been found to date in the 5 AU gap between the two outermost planets, f and d, with semimajor axes $a = 0.781$ AU and $a = 5.77$ AU, respectively.

Despite the similarities in orbital characteristics, the planetary system of 55 Cnc exhibits some conspicuous differences when compared to our solar system (Fischer et al. [2008] and Table 1): (a) Three of the planets orbit too close to the star (within 0.24 AU), that is closer than the orbit of Mercury around the Sun. (b) The second planet, 55 Cnc b ($a = 0.115$ AU), is also the second largest with a mass of 0.824 – 1.03 Jupiter masses. This planet also shows the lowest orbital eccentricity ($e = 0.014$) among all 5 planets. (c) The 4 inner planets are all quite massive, with the innermost planet, 55 Cnc e ($a = 0.038$ AU), having the smallest mass (10.8 – 13.5 Earth masses), a value roughly comparable to the mass of Uranus. Most, if not all, of these planets are expected to be gaseous giants in contrast to the terrestrial planets in our solar system.

The central star of 55 Cnc and the dynamics of its system have kept observers occupied for other reasons as well:

1. This star is the primary in a visual binary (separation $\sim 10^3$ AU) and belongs to a group of ~ 30 multiple stellar systems in which giant planets are seen orbiting very close to

¹Based on the inclination of 55 Cnc d, the inclination of the orbital plane appears to be $i = 53^\circ$ (McArthur et al. 2004), which increases all masses by 25%.

Table 1:

CHARACTERISTICS OF THE OBSERVED PLANETS
AROUND 55 CANCRI A (FISCHER ET AL. 2008)

Index i	Planet Designation	Orbital Period P_i (days)	Semimajor Axis a_i (AU)	Minimum Mass $M_{min,i}$ (M_J) ^a	Orbital Eccentricity e_i
1	e	2.817	0.038	0.034	0.070
2	b	14.65	0.115	0.824	0.014
3	c	44.34	0.240	0.169	0.086
4	f	260.0	0.781	0.144	. . . ^b
5	d	5218	5.77	3.835	0.025

NOTES:

(a) Minimum masses are given in Jupiter masses.

(b) Undetermined value, but the data are consistent with $e_4 = 0$.

the primary stars (Eggenberger et al. 2004; Raghavan et al. 2006). In fact, the most massive inner planets tend to be found in multiple stellar systems and those with the shorter periods ($P < 40$ days) tend to also have very low eccentricities. The three inner planets of 55 Cnc, with orbital periods $P = 2.82 - 44.3$ days and eccentricities $e = 0.014 - 0.086$, all fit precisely this trend.

2. The primary star of 55 Cnc has very high metallicity compared to the Sun ($Z \simeq 2Z_{\odot}$; Gonzalez & Vanture 1998; Valenti & Fischer 2005), a property that has been associated with a higher probability of forming massive protoplanetary cores and gaseous giant planets in the surrounding, also metal-rich, disk by the process of core accretion (Ida & Lin 2004b; Bodenheimer & Pollack 1986; Pollack et al. 1996).
3. It seemed for a time that an extended disk of dust was visible in the infrared, but this result was negated when additional infrared observations failed to detect a disk (Schneider et al. 2001; Bryden et al. 2006) and submillimeter observations indicated that the excess flux could be attributed to background sources (Jayawardhana et al. 2002).
4. The orbits of the two more massive of the inner planets, 55 Cnc b and c, appear to be close to but not quite in mean-motion resonance with a period ratio of nearly 3:1 (Marcy et al. 2002; Fischer et al. 2008). This is the only known 3:1 apparent resonant

pair,² whereas in all the other known cases the planets appear to have been captured in 2:1 resonances (Butler et al. 2006).

The picture that emerges from the observations of 55 Cnc is enigmatic. The most important questions can be summarized as follows (Fischer et al. 2008): Why did this star end up with so many massive planets when 90% of the observed stars do not have any giants at all? The similarities to our solar system seem to indicate that multiple-planet systems like 55 Cnc (and μ Ara³) should be common, but why have they not been observed in larger numbers? And if such multi-planet systems around metal-rich stars represent the new norm of planet evolution (Ida & Lin 2004b), where are the systems with central stars chemically similar to our Sun? One would certainly be reluctant to admit that our solar system is special because of the inherent bias associated with such a proposition. In addition, were the inner planets of 55 Cnc (and μ Ara) formed "in-situ" on the observed orbits (Lissauer 1995; Bodenheimer et al. 2000), or are they the result of inward migration (Ward & Hahn 2000; Lin et al. 2000; Armitage et al. 2002; Alibert et al. 2004, 2005a, 2006) that terminated conveniently (Marcy et al. 2000; Trilling et al. 2002; Eggenberger et al. 2004) to allow for the planets to survive and circularize their orbits? And why are all the planetary orbits in 55 Cnc so nearly circular when large eccentricities are quite common in exoplanets (Marcy et al. 2000, 2005) and it appears that resonant tidal interactions did not take hold since an actual 3:1 commensurability was not established? Finally, could there be smaller planets or an asteroid belt in the 5 AU gap and, in any case, why was matter acquisition so disparate as to produce a series of smaller planets surrounded by two very massive planets, 55 Cnc b and d? Finding answers to even some of these questions can be a giant step toward understanding planet formation and evolution. We will revisit the underlying issues in § 3.2.2 below.

1.2. Theoretical Models

The observations of 55 Cnc have motivated several empirical modeling efforts that attempted to explore the various compelling issues that arise from the impressive regularity of this planetary system, the existence of the 5 AU gap, and the unusual chemical properties

²Desort et al. (2008) have just reported another possible 3:1 resonant pair in HD 60532 that may be confirmed within the next decade.

³The metal-rich star μ Ara (HD 160691, GJ 691) also has a gaseous giant orbiting beyond 5 AU ($a = 5.235$ AU) and 3 additional giants orbiting close to the star (Santos et al. 2004; Pepe et al. 2007; and Table 5 below). Their distribution shows a large gap between 1.5 and 5.2 AU; but the orbital eccentricities of the inner planets are comparatively larger ($e = 0.067 - 0.172$) than those in 55 Cnc (see also § 3.2.3).

of the parent star:

1. *Metal-rich environment for planet formation.*— Ida & Lin (2004a, b, 2005) carried out Monte Carlo simulations of protoplanetary core growth, orbital migration, and gas acquisition. Their model predicts that the probability of forming gas giants increases rapidly with increasing metal abundances in the host stars and the surrounding disks, which is consistent with the multitude of planets observed in 55 Cnc and μ Ara. On the other hand, the physical and orbital properties of these planets are in disagreement with the main features of this model, namely that there should not be planets with 10 – 100 Earth masses at $a = 0.2 - 3$ AU and that short-period, Neptune-size planets should not be common around such G-type stars as opposed to M dwarfs. This led Ida & Lin (2005) to speculate that the planets seen in 55 Cnc and μ Ara have not migrated to their present locations but they were instead formed in-situ with the help of sweeping mean-motion or secular resonances. However, there is no evidence that gas-giant migration or resonances ever played a role in the formation of these planets, and this adds to the mystery surrounding such well-ordered planetary systems.

2. *Long-term orbital stability.*— The stability of the planetary orbits in 55 Cnc has been investigated independently by several groups: Raymond & Barnes (2005) integrated the orbits of the 3 most massive planets (b–d) for 100 Myr and found that the system could afford to have more planets in stable orbits between planets c and d. Fischer et al. (2008) integrated the orbits of all 5 planets for 1 Myr and found that planets b and c are not locked into a 3:1 mean-motion resonance. Gayon et al. (2008) integrated the orbits of all 5 planets for 400 Myr and showed that the system represents a case of stable chaos in which, however, close encounters between planets are avoided. All of these models indicate clearly that the system is dynamically stable over long time scales ($\gtrsim 0.1$ Gyr).

3. *Apparent 3:1 mean-motion resonance.*— The apparent 3:1 mean-motion resonance between the orbits of planets b and c in 55 Cnc was initially hailed as a new example of a low-order commensurability in a "resonant system" (Barnes & Quinn 2004), with 2:1 resonances providing the only previous example in observed systems. Although Barnes & Quinn (2004) did not study 55 Cnc explicitly, their models showed that planets in resonant systems have very narrow zones of stability and raised the possibility that such systems are only marginally stable. Modeling of 55 Cnc was undertaken by Zhou et al. (2008) who showed that planets b and c can be captured in a 3:1 resonance if they start with modest eccentricities ($e \sim 0.01 - 0.05$) and migrate slowly (for ~ 0.1 Myr). The above models would indicate that the arrangement of the inner planets in 55 Cnc is the result of special circumstances, an uncomfortable notion. Since we now know that planets b and c are not in resonance (Fischer et al. 2008; Gayon et al. 2008), a more palatable conjecture is that

no special migration has ever occurred in 55 Cnc and that its inner planets form a typical "interacting system" (Barnes & Quinn 2004) in which the planets are able to perturb one another and have broad zones of stability available to them.

Modeling efforts and related conjectures concerning the apparent 3:1 resonance in 55 Cnc demonstrate how difficult it is to simulate such complex systems because we do not have a handle on the initial conditions; numerical models that start from arbitrary but convenient initial conditions are capable of producing "easily" just about all of the observed results. So it is not surprising that more recent modeling efforts (although they did not address 55 Cnc directly) now seem to provide evidence against 3:1 resonant captures of planets in general: Pierens & Nelson (2008) found that massive planets captured by a dominant, Jupiter-size planet tend to end up exclusively in 2:1 or 3:2 mean-motion resonances, depending on their mass. Furthermore, Adams et al. (2008) and Lecoanet et al. (2008) found that turbulence in the host protoplanetary disk can upset mean-motion resonances and thus resonant systems should be rarely observed.

4. *Packed planetary systems hypothesis.*— The orbital stability calculations of Barnes & Quinn (2004) and related simulations by Barnes & Raymond (2004) used massless test-particles in models of several known extrasolar multiplanetary systems in order to identify broad regions full of dynamically stable orbits and to predict the possible existence of additional, yet unseen planets. These calculations were extended by Raymond & Barnes (2005), Raymond et al. (2006), and Barnes et al. (2008) to include various Saturn-mass and terrestrial-mass particles in-between the orbits of the known planets in each simulated system. Although it was easy to find stable orbits for additional planets with terrestrial or smaller masses in some of these systems, the main result of these numerical experiments came as a surprise: Many systems are on the edge of stability and small changes to the values of a or e push them to become unstable. Following the ideas of Laskar (1996), Barnes & Raymond (2004) conjectured that the remaining apparently stable systems are also packed with enough planets to be marginally stable. This is the packed planetary systems (PPS) hypothesis and it predicts that stable systems may contain unseen planets that bring them to the edge of stability. The PPS models successfully predicted the existence of HD 74156 d (Barnes et al. 2008) before its discovery (Bean et al. 2008) and proved to be consistent with the presence of 55 Cnc f that was found (Fischer et al. 2008) orbiting at the inner edge of the predicted stable zone ($0.7 \text{ AU} < a < 3.2 \text{ AU}$, $e < 0.2$; Barnes & Raymond 2004).

The stable zone in 55 Cnc is too wide, as a result the 5-planet system is still not packed and there could be more undetected planets between the planets f and d (Raymond et al. 2008). Specifically, the PPS models suggest the following interesting possibilities: (a) A giant planet with up to Saturn mass may exist near 2 AU (the center of the stable zone)

with $e \sim 0.08$ (Raymond & Barnes 2005). (b) Alternatively, several terrestrial planets with up to 0.63 Earth masses may exist at 1.1–3.6 AU with $e \leq 0.36$ (Raymond et al. 2006). Although the possibility of having Earth-like planets in the ”habitable zone” around 1 AU is intriguing, our own interest in this work is focused entirely on the possibility of having a gas giant orbiting at ~ 2 AU for the reasons that we explain in § 1.3 below. The current observations of 55 Cnc do not rule out such a planet: At a distance of ~ 2 AU, a giant planet could avoid detection if its minimum mass is smaller than 100 Earth masses (Fischer et al. 2008), i.e., approximately equal to or less than the mass of Saturn.

5. *Empirical Titius–Bode relation.*— Poveda & Lara (2008) presented an exponential fit of the semimajor axes of the 5 known planets in 55 Cnc. This empirical relation is akin to the Titius–Bode (TB) rule for the solar system, but it works only if there exists a hypothetical sixth planet at $a = 2.08$ AU. Based on this result, Poveda & Lara (2008) proposed that an unseen planet with $a \approx 2$ AU should be present in 55 Cnc. There is no physical basis for this prediction, yet it is quite interesting that the empirical TB relation of 55 Cnc is in complete agreement with the prediction of the PPS model for a gas giant at the same orbital distance.

Since the PPS model and the TB relation converge to the same prediction, they can both be tested by additional Doppler–shift measurements of the primary star of 55 Cnc. By extending their baseline, future observations should be able to search for an additional periodicity in the 5 AU gap of 55 Cnc and, irrespective of the outcome, the result can be pivotal for planet formation theories (see also § 1.3.5).

6. *The protoplanetary disk of 55 Cnc.*— Fischer et al. (2008) made an attempt to estimate some key parameters of the minimum–mass protoplanetary disk of 55 Cnc. Using a typical surface density profile for the disk that varied with distance R as $\Sigma(R) \propto R^{-3/2}$ and an estimate of the core masses of the 5 observed planets that took into account the excessive metallicity of the system, they found a total mass of $0.031 M_{\odot}$ out to 6 AU and a surface density for the dust of 8.7 g cm^{-2} at 5 AU. The dust-to-gas mass ratio was set to the nominal value of 1% and the mass estimate also took into account the intermediate inclination of the orbital plane of the system ($i = 53^{\circ}$, as derived by McArthur et al. [2004] for 55 Cnc d).

The assumed $\Sigma(R)$ profile was first established for the minimum–mass solar nebula (MMSN) by Weidenschilling (1977) and Hayashi (1981) and it has been commonly used ever since in calculations of this type. Recently, this profile was investigated again in our solar system (Davis 2005), in extrasolar systems (Kuchner 2004), and in dusty circumstellar disks around T Tauri stars (Kitamura et al. 2002; Andrews & Williams 2007). Due to large systematic uncertainties, none of these investigations has been able to directly confirm or reject the original $\Sigma(R)$ relation, although all of them provide useful hints about possible

improvements of the "typical" surface density profile of the solar nebula and extrasolar protoplanetary disks. For what follows, it is interesting to note that the the model of Davis (2005) indicates that the original power-law $\Sigma \propto R^k$ with $k = -3/2$ tends to overestimate the surface density within the central 1 AU of the solar nebula. Also, Kuchner (2004) finds a steeper profile with $k = -2$ for the surface density of the typical minimum-mass "extrasolar nebula" (MMEN) constructed by Weidenschilling's (1977) method from 26 exoplanets found in multi-planet systems. The $k = -2$ power-law index results, again, in an overestimate of the surface density within the central 1 AU of the MMEN. The lack of a central core region, such as that suggested for the MMSN (Lissauer 1987; Davis 2005) and for circumstellar disks (Garaud & Lin 2007), is the obvious reason for the excessive central densities in models that adopt a single power-law density profile for the entire protoplanetary disk.

1.3. A New Theoretical Model

We are interested in 55 Cnc because this is the only extrasolar system with so many planets in well-ordered, long-lived, circular orbits. We believe that the high degree of regularity seen in this system makes it an ideal laboratory for exploring the above-discussed issues and for testing the leading current hypotheses and models about planet formation in protostellar disks.

Our work starts with a new physical model that we formulated rigorously based on exact solutions of the isothermal Lane-Emden equation with rotation and that relates the observed planets in a well-ordered, multi-planet system to key physical properties of the protoplanetary disk that hosted their formation. First we applied this model successfully to the 11 largest planets of our solar system (Christodoulou & Kazanas 2008, hereafter CK) and we proceed here to apply it to the 5 known planets of 55 Cnc.

The results obtained from our modeling are tied to the theoretical models of § 1.2 in the following ways:

1. Our model uses all the planets in regular orbits irrespective of size, mass, and metal abundances. As such, it works equally well for solar-type systems like our solar system and for systems with different metallicities or with gas giants in short-period orbits like 55 Cnc. We do expect however that the modeling results will have to be interpreted consistently with the physical and the chemical properties of the detected planets and their parent stars.
2. It is important that the planetary orbits of 55 Cnc were found to be dynamically stable over long time scales because our model associates such long-lived orbits with local

minima of the gravitational potential well in the midplane of the original protoplanetary disk. This association does not hold for many odd systems in which one or two planets have migrated inward and are now seen very close to their parent stars. However, the regular spacing of the planets and the stability of 55 Cnc argue against migration as a process that dominated its evolution.

3. It is now clear that 55 Cnc b and c are not caught in a 3:1 mean–motion resonance. This result also suggests that no significant migration has taken place in the disk of 55 Cnc and it supports our picture of a well-ordered system in which the planets formed in–situ by core accretion. In turn, such regular planetary orbits readily provide information about the locations of density enhancements (the local potential minima) in the disk during the planet formation stage.
4. The PPS models predict that there must exist at least one more planet in the 5 AU gap of 55 Cnc and they will be tested by future observations for the first time in such a well-ordered, multi-planet, extrasolar system. Our model is also not impervious to the possible existence of an additional planet, but it does not necessarily need a 6th planet in order to work. As it predicts entirely different physical characteristics for the disk of 55 Cnc depending on whether 5 or 6 planets are used (see § 2.4), our model too needs an observational resolution of this dilemma.
5. Based on the work of CK, we now understand that the TB relation can be accommodated within our approach, but the rule has no inherent physical significance for our solar system or for 55 Cnc. Since the TB relation of 55 Cnc necessarily predicts a 6th planet at $a \approx 2$ AU, the absence of such a planet from the 5 AU gap will settle this issue without a doubt. Such an observational result will however be detrimental to the PPS hypothesis as well. Alternatively, if an additional planet is found in the 5 AU gap, then the doubts will persist, the PPS hypothesis will persevere, and our model (and presumably models such as those of Weidenschilling [1977] and Davis [2005]) will then show a clear preference for a different radial density profile of the protoplanetary disk of 55 Cnc (see § 2.4 for details).
6. The attempt of Fischer et al. (2008) to estimate some of the properties of the minimum–mass protoplanetary nebula (MMPN) of 55 Cnc is noteworthy by insufficient. The main drawback of these estimates is that the authors assumed a $\Sigma \propto R^{-3/2}$ profile for the disk without actually using Weidenschilling’s (1977) method or any of the competing methods cited in § 1.2.6 above. Consequently, the particular density profile produced by our disk model of 55 Cnc cannot be compared to this previous work. Some of the parameter values obtained by Fischer et al. (2008) and by Kuchner (2004), who did

use Weidenschilling’s method, can however be compared to the results of our modeling, and we do so in § 2.5 below.

1.4. Outline

In § 2, we describe in detail the new physical model of the midplane of the protoplanetary disk of 55 Cnc and we derive the fundamental dynamical parameters of this disk (minimum mass, density profile, specific angular momentum, rotation frequency, and equation of state). We also examine the dynamical stability of the model and we describe the effects that a possible 6th planet will have if it is discovered orbiting at $a \approx 2$ AU, as expected by the PPS and TB models of the system (§ 1.2).

In § 3, we interpret the results from our model and we discuss the issues and the questions mentioned above that pertain to the impressive regular structure of this planetary system and its intriguing 5 AU gap. We also report briefly on our modeling effort of the related multi-planet system μ Ara.

2. Physical Model of the Protoplanetary Disk of 55 Cnc

2.1. Basic Equations

We are interested in the equilibrium structure of a rotating, self-gravitating, isothermal disk of angular velocity Ω , mass density ρ , and sound speed c_0 . Following CK, we adopt cylindrical coordinates (R, ϕ, z) , the assumption of axisymmetry ($\partial/\partial\phi = 0$), and the assumption of cylindrical symmetry ($\partial/\partial z = 0$) that is valid on the midplane of any disk. We cast all quantities in dimensionless form as follows: We use the central density $\rho_0 \equiv \rho(0)$ and the length scale of the disk

$$R_0 \equiv \frac{c_0}{\sqrt{4\pi G\rho_0}}, \quad (1)$$

where G is the gravitational constant, and we define the normalized radius as $x \equiv R/R_0$ and the normalized density as $\tau \equiv \rho/\rho_0$. In addition, we adopt a rotation profile of the form

$$\Omega(R) = \Omega_0 f(x), \quad (2)$$

where $\Omega_0 \equiv \Omega(0)$ and the dimensionless function $f(x)$ is to be determined. Finally, we use Ω_0 and the Jeans frequency $\Omega_J \equiv \sqrt{2\pi G\rho_0}$ to define a dimensionless rotation parameter of the form

$$\beta_0 \equiv \frac{\Omega_0}{\Omega_J}. \quad (3)$$

The equilibrium structure of the midplane of the disk is then described by the isothermal Lane–Emden equation with rotation that takes the dimensionless form

$$\frac{1}{x} \frac{d}{dx} x \frac{d}{dx} \ln \tau + \tau = \frac{\beta_0^2}{2x} \frac{d}{dx} (x^2 f^2) . \quad (4)$$

In CK, we showed that any power–law density profile is an exact analytic solution of this equation, provided that the rotation profile $f(x)$ is also determined self–consistently from eq. (4). Such ”baseline” power–law profiles are particular solutions of the Lane–Emden equation, but they are unable to satisfy the central boundary conditions, namely that

$$\left\{ \begin{array}{l} \tau(0) = 1 \\ \frac{d\tau}{dx}(0) = 0 \end{array} \right\} . \quad (5)$$

They do however determine analytically the appropriate rotation profile $f(x)$ and the mean density profile irrespective of the applicable (physical) boundary conditions. The exact solutions can then be obtained by a simple numerical integration that obeys the boundary conditions (5), and they are bound to oscillate permanently about the corresponding baseline solutions without ever settling on to them (that would be a violation of the boundary conditions). It is important to note that, although any monotonic power–law profile can be chosen as a baseline solution and it will produce a monotonic rotation profile, the corresponding exact solution subject to the boundary conditions (5) will still have to be oscillatory, creating thus a series of local maxima and minima across the entire density profile.

2.2. Baseline Model

For our baseline equilibrium model of the midplane of the MMPN of 55 Cnc, we adopt a composite analytic solution in which the mean density profile is a combination of a flat inner region (a ”core”) followed by a declining power–law:

$$\tau_{base}(x) = \beta_0^2 \cdot \left\{ \begin{array}{ll} 1 , & \text{if } x \leq x_1 \\ (x_1/x)^\delta , & \text{if } x > x_1 \end{array} \right. , \quad (6)$$

where x_1 is the radius of the constant–density core region and $\delta > 2$. Compared to the model of the solar nebula in CK, this model does not have a flat outer region because no outer equidistant planets are observed in 55 Cnc.

The rotation profile is determined next by substituting eq. (6) into eq. (4) and by solving

the resulting differential equation:

$$f(x) = \begin{cases} 1, & \text{if } x \leq x_1 \\ \sqrt{\frac{1}{\delta-2} [\delta (x_1/x)^2 - 2 (x_1/x)^\delta]}, & \text{if } x > x_1 \end{cases}. \quad (7)$$

It is easy to show that this rotation law obeys the physical requirements that $f(x) > 0$ and $df/dx \leq 0$ everywhere for any choice of $\delta > 2$.

The functions $\tau_{base}(x)/\beta_o^2$ and $f(x)$ are plotted in Figure 1 for $x_1 = 100$ and for various choices of the power-law index $\delta > 2$. We see that, as δ is increased, the rotation profile is not affected as much as the density profile.

2.3. Solutions of the Boundary-Value Problem and Parameter Optimization

The above composite equilibrium model is characterized by three free parameters: the core radius $x_1 > 0$, the rotation parameter $\beta_0 \leq 1$, and the power-law index $\delta > 2$. The density profile (eq. [6]) of this baseline solution of the Lane–Emden equation (4) is not capable of satisfying the physical boundary conditions (5) at the center and it serves only as a mean approximation to the mean density of the corresponding physical model. The general form of the rotation law of the baseline (eq. [7]) can, however, be adopted for the differential rotation $f(x)$ of the physical model as well. Then eq. (6) provides a prescription for the RHS of the Lane–Emden equation (4) which can thus be written as

$$\frac{1}{x} \frac{d}{dx} x \frac{d}{dx} \ln \tau + \tau = \tau_{base}(x). \quad (8)$$

This differential equation can be integrated numerically subject to the physical boundary conditions (5). For all choices of the free parameters $\{x_1 > 0, \beta_0 \leq 1, \delta > 2\}$, the numerical solutions oscillate about the baseline solutions (6). The local maxima of the density profile correspond to minima of the gravitational potential well in the midplane of the disk and they are ideal locations for the formation of planetary cores from the dust grains that also have to aggregate inside these wells.

We construct a model of the MMPN of 55 Cnc by choosing the 3rd planet ($a = 0.240$ AU) from the star to set the physical scale of the model. (Similar results are obtained when any of the inner 4 planetary orbits is used for scaling.) Then the third density peak of the model (not counting the central peak at $x = 0$) is associated with a distance of 0.24 AU from the center, and the exact solutions of the Lane–Emden equation (8) are optimized by varying the free parameters until the remaining density enhancements match as closely as possible the

Table 2:

DENSITY PEAKS
IN THE BEST-FIT MODEL
OF THE MMPN OF 55 CNC

Index	Planet	Semimajor	Peak	Relative	Peak
i	Designation	Axis	Location	Deviation	Density
		a_i (AU)	d_i (AU)	(%)	$\tau(d_i)$
1	e	0.038	0.042	10.5	4.302×10^{-2}
2	b	0.115	0.091	-20.9	8.076×10^{-3}
3	c	0.240	0.240	. . .	7.743×10^{-4}
4	f	0.781	0.862	10.4	3.561×10^{-5}
5	d	5.77	5.61	-2.8	3.855×10^{-7}

observed semimajor axes of the remaining planetary orbits of 55 Cnc. The best-fit model is shown in Figure 2 and its density peaks are listed in Table 2 along with the observed semimajor axes given by Fischer et al. (2008). The third density peak occurs at $x = 316.91$ in the best-fit model of 55 Cnc, implying that the length scale of the protoplanetary disk in the isothermal phase of its evolution was extremely small ($R_0 = 7.573 \times 10^{-4}$ AU). This value is ~ 30 times smaller than the length scale of our solar system ($R_0 = 2.244 \times 10^{-2}$ AU; CK) and indicates that the inner disk of 55 Cnc was denser than the solar nebula (see § 2.4 below). Furthermore, there is no other density peak out to 100 AU, so this model predicts no more planets beyond the orbit of 55 Cnc d.

The relative deviations between the locations of the model peaks and the planetary orbits are also listed in Table 2. The largest relative deviation ($\sim 21\%$) is observed for the second peak that corresponds to the orbit of planet b. This difference is still quite small (~ 0.02 AU) in absolute terms but it appears disproportionately large because our method of optimization is skewed toward the inner planets for which it produces larger relative deviations (see CK for more details). The values listed in Table 2 cannot be improved individually because of the extreme nonlinear nature of the problem. Only the value of β_0 can be optimized independently of the other parameters by minimizing the deviation of the innermost planet from the corresponding density peak. The strong coupling of the remaining two parameters then demonstrates that fitting 5 planetary orbits with 3 free parameters is not a simple matter, as nonlinearities do not generally allow for one-to-one relations between parameters and planetary positions.

2.4. Physical Properties

The parameters of the best-fit model determined by the optimizing algorithm along with the scaling assumption that $d_3 = 0.24$ AU (see Table 2) constitute a set of important dynamical parameters of the MMPN of 55 Cnc:

$$\left\{ \begin{array}{l} \delta = 2.4708 \\ \beta_0 = 0.1228 \\ x_1 = 69.10 \\ R_0 = 7.573 \times 10^{-4} \text{ AU} \\ R_1 \equiv x_1 R_0 = 5.233 \times 10^{-2} \text{ AU} \end{array} \right\}. \quad (9)$$

The value of the power-law index $\delta \approx 2.5$ indicates that the density profile of the differentially-rotating region of the disk declined with radius, on average, as $R^{-2.5}$. This region extended outward beyond the core radius of $R_1 \approx 0.05$ AU. The low value of β_0 indicates that the rotation of the isothermal nebula was sufficiently slow to avoid nonaxisymmetric instabilities (see § 2.6 below). The unusually small value of R_0 , along with eq. (1) and a typical low gas temperature, indicates that the nebula was very dense, about $\sim 10^3$ times denser than the solar nebula (see Table 3 below). So the picture that emerges from the best-fit model of 55 Cnc is that of a relatively heavy and slowly rotating disk that is long-lived and that can comfortably build massive planets over time by accumulating the solids and then accreting the gas contained within each local potential well.

The optimization procedure also finds some models of high quality in which somewhat larger magnitudes of β_0 are compensated by smaller values of x_1 . The most different model gives us an idea about how shallow the area around the true minimum is in the three-parameter space of the model. This model is characterized by the following values: $\delta = 2.4710$, $\beta_0 = 0.1583$, $R_0 = 9.839 \times 10^{-4}$ AU, $x_1 = 52.66$, $R_1 = 5.181 \times 10^{-2}$ AU, and the relative deviations are smaller than 22%. However, the power-law index does not differ from $\delta = 2.5$ by more than 1.2% in any of the high-quality models. Similarly, the variations of R_0 and x_1 always produce core radii to within 1% of $R_1 = 0.052$ AU in all of these models, so there is no doubt that the core region of the MMPN of 55 Cnc was extremely small (~ 10 solar radii).

The Lane-Emden equation that we solved can serve as a model of a differentially-rotating disk supported by thermal pressure in the z -direction, so we expect that the scale height from pressure support will be $H \propto R$ down the radial density gradient.⁴ In this case,

⁴The vertical scale height of a pressure-supported disk is

$$H \sim \frac{c_0}{\Omega} \sim \frac{c_0}{v} R,$$

the value of $\delta \approx 2.5$ implies that the corresponding power-law index in the surface-density profile ($\Sigma \propto R^{-\delta+1}$) of the nebular disk was $k = 1 - \delta \approx -1.5$. This value is virtually identical to that obtained for the solar nebula by Weidenschilling (1977) who used an entirely different method and by CK who used the same optimization technique as in this work.

The conformance of these results does not hold if a 6th planet is assumed to exist in the 5 AU gap of 55 Cnc. We have also optimized models that included a hypothetical planet at $a = 2$ AU (as predicted by the PPS and TB models of 55 Cnc), and the best-fit model of the six planetary orbits has the following parameter values: $\delta = 2.1174$, $\beta_0 = 0.1334$, $R_0 = 7.511 \times 10^{-4}$ AU, $x_1 = 56.02$, $R_1 = 4.208 \times 10^{-2}$ AU, and the relative deviations are smaller than 19%. These values are comparable to those in the best-fit model of the 5 observed planets, except for δ whose smaller value produces a softer density gradient to accommodate the hypothetical planet at 2 AU. This softer gradient can also accommodate one additional planet farther out, but the outermost density peak occurs at 20.56 AU which differs from $a \approx 15$ AU predicted for a hypothetical 7th planet by the empirical TB relation of Poveda & Lara (2008). This peak is also not consistent with the recent PPS prediction (Raymond et al. 2008) that an unseen outer planet could exist close to 9 or 10 AU, i.e. near the inner edge of a wide zone of stability found beyond 55 Cnc d. Thus, our model with hypothetical planets is still markedly different than the PPS and TB models of 55 Cnc.

Our modeling also delineates some of the fundamental physical characteristics behind the mean density profile of the midplane of the disk of 55 Cnc. With the aid of our best-fit model, we can deduce substantial information concerning the structure and the dynamics of the nebular disk. In addition to the structural and rotational parameters discussed above, we can use our analytic baseline model in order to probe the dynamical state of the protoplanetary disk of 55 Cnc in its isothermal phase. Following CK, we calculate the relevant physical quantities for the MMPN of 55 Cnc and we summarize our results in Table 3.

The corresponding results obtained by CK for the solar nebula are also listed in Table 3 for comparison purposes. Compared to the core of the solar nebula, the MMPN core of 55 Cnc was smaller (R_1 ratio ~ 16), denser (ρ_0 ratio $\sim 10^3$), heavier (Ω_J ratio ~ 30), and it was rotating ~ 10 times faster. The disk contained ~ 100 times less mass⁵ within a 6-AU radius

where v is the rotation speed. In our models, v becomes asymptotically flat when the density exhibits a power-law profile with $\delta > 2$ and c_0 is constant, leading to the approximate relation that $H \propto R$.

⁵ The mass content of both models is considerably smaller than that of the MMSN because we consider only the mass within one length scale from the midplane of each disk (i.e., for $|z| \leq R_0$) and R_0 is extremely small in both cases. The z -integration needs to be extended for about 1 AU away from the midplane in order to produce masses $\sim 0.01 M_\odot$.

Table 3:

PHYSICAL QUANTITIES OF THE NEBULAR DISKS
OF 55 Cnc AND THE SOLAR SYSTEM

Description	Quantity	55 Cnc Value ^a	Solar System Value ^a
Equation of State	$c_0^2/\rho_0 = 4\pi GR_0^2$	= 1.08×10^{14}	9.45×10^{16}
	$\bar{\mu} \rho_0/T$	= 7.73×10^{-7}	8.80×10^{-10}
Central Density ^b	ρ_0	= 3.30×10^{-6}	3.76×10^{-9}
Jeans Frequency	$\Omega_J = \sqrt{2\pi G\rho_0}$	= 1.18×10^{-6}	3.97×10^{-8}
Rotation Frequency	Ω_0	= 1.44×10^{-7}	1.65×10^{-8}
Rotation Period	$2\pi/\Omega_0$	= 1.4 yr	12 yr
Core: $R \leq R_1, z \leq R_0$ ^c			
Surface Density	$\Sigma_0 = 2R_0\rho_0$	= 74800	2520
Mass	M_1	= $10^{-6} M_\odot$	$10^{-4} M_\odot$
Specific Angular Momentum	$L_1/M_1 = \Omega_0 R_0^2 x_1^2 / 2\beta_0^2$	= 2.94×10^{18}	7.19×10^{18}
Disk: $R \leq 6 \text{ AU}, z \leq R_0$ ^c			
Mass	M	= $5 \times 10^{-6} M_\odot$	$4 \times 10^{-4} M_\odot$

NOTES:

(a) cgs units apply unless stated otherwise.

(b) $T = 10 \text{ K}$ (gas temperature) and $\bar{\mu} = 2.34 \text{ g mol}^{-1}$ (mean molecular weight) assumed.

(c) R_0 and R_1 are smaller in 55 Cnc by factors of ~ 30 and ~ 16 , respectively.

and only 2/5 of the angular momentum per unit mass. There is no doubt that these two disks were different and their differences are reflected in the distributions and the physical properties of the various planets that they formed over time.

2.5. Surface Density Profile

Using the Σ_0 value of 55 Cnc from Table 3, the core radius $R_1 = 0.05233 \text{ AU}$, and the power-law index $k \approx -1.5$, we can write the surface density profile of the MMPN of 55 Cnc

for $R \geq R_1$ in the form

$$\Sigma(R) = 895 \left(\frac{R}{1 \text{ AU}} \right)^{-1.5} \text{ g cm}^{-2}, \quad (10)$$

where R is measured in AU. This equation shows that the surface density of the gas is $\Sigma = 895 \text{ g cm}^{-2}$ at $R = 1 \text{ AU}$ and $\Sigma = 80 \text{ g cm}^{-2}$ at $R = 5 \text{ AU}$. These values are 48% of the corresponding values in the solar nebula.

The 1-AU value is in agreement with Kuchner’s (2004) result of 739 g cm^{-2} , although he used just the 3 planets b–d, the only ones known at the time. In particular, planet f was not included in the model and this is the reason that the 1-AU value was underestimated and the density profile turned out to be too steep with $k = -2.42$. In general, undetected planets cause the main problem in this method, and if such planets are included, they tend to soften the density gradients and push Kuchner’s average MMEN value of $k = -2$ closer toward -1.5 .

The 5-AU value corresponds to a typical surface density of solids of 1 g cm^{-2} for a nominal value of 1% for the dust-to-gas mass ratio. This value is comparable to the low-end values calculated by Fischer et al. (2008) using only the planetary masses inferred from observations. Some additional estimates by the same authors reach as high as 8.7 g cm^{-2} . Such estimates rely on uncertain assumptions about the masses of the solid planetary cores and they are obviously too high, as they predict much larger densities in the disk of 55 Cnc compared to those in the solar nebula. But we believe that the opposite is true since our model and Kuchner’s (2004) model, following entirely different methodologies, both predict significantly lower densities at 5 AU for the MMPN of 55 Cnc than the MMSN. We note that such low densities in the outer disk of 55 Cnc do not pose a problem for the formation of the massive planet d. As Fig. 2 shows, the half-width of the corresponding density peak is about 3 AU, and all the solids within this enormous potential well were bound to aggregate at the bottom and form the massive core of this planet.

2.6. Dynamical Stability

All composite power-law models with $\delta > 2$ described above are stable to axisymmetric perturbations because they satisfy the Rayleigh criterion: The specific angular momentum ΩR^2 is an increasing function of R at all radii. This can be shown easily by using eq. (7) to provide the function f^2 and then by proving that $d(f^2 x^4)/dx \geq 0$ for all x and $\delta > 2$.

The above models are also stable to nonaxisymmetric perturbations because they do not rotate too fast. For sufficiently slow rotation, the nonaxisymmetric modes are neutral and

incapable of merging to produce instability. This behavior is captured in the α -parameter stability criterion (Christodoulou et al. 1995) which for gaseous disk models can be written as

$$\alpha \equiv \frac{1}{2} \left(\frac{\Omega_0}{\Omega_J} \right) \leq 0.35. \quad (11)$$

In our notation, this is equivalent to requiring that $\beta_0 \leq 0.7$ for stability, thus our best-fit model with $\beta_0 \approx 0.12$ is far from the threshold of nonaxisymmetric instability. A disk of dust would also be stable with this rotation law. For an unisotropic disk of particles, the corresponding stability threshold switches from 0.35 to 0.25, and the requirement for stability then becomes $\beta_0 \leq 0.5$.

3. Summary and Discussion

3.1. Summary

In § 1, we placed in proper context all the available information about the multi-planetary system of 55 Cnc. Our knowledge of this system comes from 18 years of Doppler-shift observations of the central star (Fischer et al. 2008; McArthur et al. 2004; Marcy et al. 2002; Butler et al. 1997) and from theoretical modeling of the inferred planetary orbits (Fischer et al. 2008; Raymond et al. 2008; Poveda & Lara 2008; Gayon et al. 2008; Zhou et al. 2008; Raymond & Barnes 2005; Ida & Lin 2005; Kuchner 2004). The metal-rich primary star of 55 Cnc has 5 massive planets in remarkably circular orbits and, outside of our Sun, this is the only star with so many planets in well-ordered, perfectly stable, nonresonant orbits (Table 1). The system does however exhibit a large 5 AU gap between its two outermost planets and this vast empty region has sparked speculation that one or more additional planets may still remain undetected between planets f ($a = 0.781$ AU) and d ($a = 5.77$ AU).

Our contribution to the investigation of 55 Cnc is a new physical model of the midplane of the protoplanetary disk in which the planets were formed. This model was introduced in § 1.3 and it was described in detail in § 2. It is based on exact solutions of the isothermal Lane-Emden equation with rotation (eq. [4]) subject to the appropriate central boundary conditions (eq. [5]). These solutions describe radial density profiles that are oscillatory by nature, despite the fact that the corresponding rotation profiles are strictly monotonic and well-behaved. The oscillations occur about an average (baseline) density (eq. [6]) that is a combination of two power laws, a flat uniform core and a decreasing outer section (§ 2.2). Such baseline density profiles are also exact intrinsic solutions of the Lane-Emden equation but they are incapable of satisfying the central boundary conditions (see CK for more details

and for an application of the model to our solar system). The baselines do however obey the same rotation law (eq. [7]) as the corresponding oscillatory solutions. Some typical baselines and their rotation profiles are shown in Fig. 1, while a typical oscillatory solution and its baseline are shown in Fig. 2.

The oscillatory density profile shown in Fig. 2 represents the best-fit model for the midplane of the protoplanetary disk of 55 Cnc. The fit was obtained by nonlinear unconstrained optimization that matches the orbital semimajor axes of the observed planets to consecutive density maxima (or gravitational potential minima) of the oscillatory profile (see § 2.3 and Table 2) and that uses the semimajor axis of the third planet from the star to set the physical scale of the model. The dynamical parameters of the best-fit model are listed in eq. (9) and its physical properties are summarized in §§ 2.4–2.5 and in Table 3. The midplane of the disk of 55 Cnc was composed of a very small (~ 0.05 AU) and very dense ($\sim 10^{-6}$ g cm $^{-3}$) uniform core in slow rotation (period ~ 1 yr), followed by a power-law gradient such that the surface density varied with distance as $R^{-1.5}$ (eq. [10]) out to ~ 6 AU. This configuration is stable to both axisymmetric and nonaxisymmetric perturbations (§ 2.6).

3.2. Discussion

3.2.1. *The Two Modes of Multi-planet Formation*

The $R^{-1.5}$ dependence of the surface density profile of 55 Cnc is effectively identical to that found by CK for the solar nebula. Despite this resemblance, the detailed comparison between the two nebular disks shown in Table 3 indicates that the two models are generally dissimilar, and the differences seen in Table 3 are also reflected in the differing characteristics of the planetary systems that were created around these two stars. Specifically, the inner disk of 55 Cnc was denser and heavier, and this explains why 4 massive planets were formed within the inner 0.8 AU. These high densities are also responsible for the large growth of the second planet from the star, 55 Cnc b, which is the most massive of the inner 4 planets. This planet was free to grow in a high-density environment, while the area around the orbit of the first planet could have been depleted by the protostar (just as Mercury’s growth was severely limited by the protosun). On the other hand, the same disk showed much smaller densities beyond 2 AU, and this explains why only one massive planet managed to form at the bottom of the single, very wide potential well outside of 5 AU.

The planetary system of 55 Cnc and the solar system are both remarkably well-ordered despite the differences in structure and dynamical characteristics and the differences between their host stars. This comparison seems to indicate that there exist two modes of planet

formation that lead to stable, well-organized, multi-planet systems. Based on our modeling and on the results of CK, we can describe these two extremes of multiple planet formation in the isothermal regime of protostellar collapse as follows (see also Table 4):

1. *Large Light Disks.*—Solar-type protoplanetary disks with ~ 1 AU cores and moderate rotational support (no more than $\sim 40\%$ – 50% of maximum rotation) that have core densities a few times above those required to form planets ($\sim 10^{-9}$ g cm $^{-3}$; Lissauer 1993) are capable of forming rocky planets in the first 2 AU and, due to the comparatively high densities in their outer regions, several gas giants beyond 5 AU as well. Such disks can extend for at least 40–70 AU in the radial direction. Because their core densities are barely supercritical, these disks can form only terrestrial planets in the vicinity of the core radius.
2. *Small Heavy Disks.*—Metal-rich protoplanetary disks with ~ 0.05 AU cores and little rotational support (no more than $\sim 10\%$ – 15% of maximum rotation) that have core densities ~ 1000 times above the critical value are capable of forming giant planets in the first 2 AU and, due to the substantial density drop in their outer regions, only one gas giant beyond 5 AU.⁶ Such disks cannot extend for more than 6–10 AU (and if they do, their densities are too low to form giant planets). Because their core densities are strongly supercritical, these disks can easily form gas giants around 1 AU, so terrestrial planets are not expected to be present in the habitable zone in this mode.

3.2.2. Important Questions and Feasible Answers

Returning now to the questions posed in § 1.1, we can outline some feasible answers suggested by the above results: Most of the observed stars ($\sim 90\%$) do not show any giant planets at all. Some of them, especially those of solar type, may have planetary systems formed in large light disks (LLDs), in which case their planets are not observable yet with the current resolution because the inner planets have very low masses and the outer planets are too distant from their stars. This is probably the reason why the solar system is currently the only example of a system formed in an LLD. On the other hand, the inner giant planets formed in small heavy disks (SHDs) can be presently detected. Besides the standard example of 55 Cnc, all other planets found within 2–3 AU from their stars in nearly circular orbits are

⁶On the opposite end of chemical abundances, small and heavy, metal-poor disks are not expected to form any gas giants beyond the inner few AU. A possible example is HD 37124 (Vogt et al. 2005), a system with 3 giant planets close to the star that was singled out by CK as the only other well-ordered multi-planet system besides 55 Cnc. In HD 37124, there has been no indication of a planet beyond the inner 3 AU.

good candidates for the SHD mode. This also includes μ Ara, HD 37124, and the massive, short-period ($P < 40$ days) planets with low eccentricities found in multiple stellar systems (see § 1.1).

On the question of in-situ formation versus migration, the slow rotation found in our models (Table 4) and the structure of the disks that show several local potential minima strongly support the in-situ formation of planets by planetesimal aggregation and gas accretion inside these potential wells. This does not mean that planetary migration cannot occur at all, it just indicates that the multiple planets of well-ordered systems do not migrate. Migration may still be the dominant mechanism in systems with planets in highly eccentric and/or irregularly spaced orbits. But even in such cases, our modeling adds a new dimension to the migration problem that has not been previously explored: The ability of a planet to migrate can no longer be determined solely by the disk torques that redistribute the angular momentum of a planetary orbit. That was done in the past (e.g., Lin et al. [2000], Ward & Hahn [2000], and references therein) while the density profile of the underlying disk was assumed to be monotonically decreasing without any localized potential wells. In the present setting in which the planets are trapped inside gravitational potential minima, the energy content of each planet needs to be considered as well. A planet orbiting inside a local gravitational potential well can migrate only if the interaction with the disk provides enough energy for it to leap out of its well—otherwise the torqing of the planetary orbit will simply lead to stable oscillations and the development of some eccentricity inside this potential minimum.

On the question of the existence of additional planets in 55 Cnc, our model boldly predicts that no other planet will be found in the future. In particular, we do not believe that there is room in the 5 AU gap even for a small rocky terrestrial planet or an asteroid belt because the potential minima of planets f and d reach into the gap (see Fig. 2), and all debris must have been swept by these two massive planets. This prediction is in contrast to the predictions of the PPS models (Raymond et al. 2008) and the TB conjecture (Poveda & Lara 2008) for the system, and the disagreement can be resolved by future observations of 55 Cnc (see also § 2.4 above).

The question of the impressive growth of inner planet 55 Cnc b ($a = 0.115$ AU, mass $0.82 - 1.0$ Jupiter masses) was discussed briefly in § 3.2.1 above. The density of the peak where this planet was formed (Table 2) is quite high ($\rho_2 = 8 \times 10^{-3} \rho_0 \approx 3 \times 10^{-8}$ g cm $^{-3}$). Only planet e was formed in a higher-density environment in the SHD of 55 Cnc, but this planet resides deep inside the core of the nebula and its gaseous envelope could have easily been ablated by the protostar at a later time. The situation is similar in the inner solar system, although Venus is slightly less massive than the Earth. The emerging paradigm,

valid for both LLDs and SHDs, is that of a depleted innermost planet followed by planets that are free to grow as much as the local conditions in the disk would allow. This picture appears to be borne out also in another SHD candidate, μ Ara, but with some caveats that we discuss below.

3.2.3. *The SHD of μ Ara*

Recent observations (Pepe et al. [2007] and Table 5) of the metal-rich star μ Ara ($Z \simeq 2Z_{\odot}$; Santos et al. 2004) indicate 4 orbiting planets in a configuration very similar to that of 55 Cnc: A single massive outer planet, μ Ara e, is separated from the 3 inner planets (c, d, and b) by a large empty region between 1.5 and 5.2 AU. The minimum mass of the innermost planet is comparable to that of the innermost planet in 55 Cnc, so this planet is also a low-mass (depleted) giant while its two neighbors have minimum masses comparable to the mass of Jupiter.

Although the eccentricities of its planetary orbits are larger than those of 55 Cnc (see Tables 1 and 5), μ Ara appears to be a good example of an SHD system. The size of the system is also comparable to that of 55 Cnc (~ 6 AU), so we expected our best-fit model to produce parameter values similar to those of 55 Cnc. We also thought that, by analogy, a PPS model of the system would find a stable zone in the 3.7 AU gap between planets b and e, and a TB model would predict a planet in the same gap. Such models are not yet available, but the TB relation of Poveda & Lara (2008) can be easily applied to the observed semimajor axes. It turns out that the TB models are not particularly good fits to the data with or without a hypothetical 5th planet in the 3.7 AU gap.

The planetary orbits of μ Ara shown in Table 5 cannot be matched to the density maxima in any of our models. The reason for this failure is that planet d is too close to planet b, and this leaves an inconspicuous 0.8 AU gap in the distribution between planets c and d. A hypothetical planet is needed in this gap to restore the regular spacing of the inner planets. This, of course, does not mean that an undetected planet necessarily exists in the 0.8 AU gap, it just implies that a density maximum is needed in that area of the model for the distribution to be typical of a well-organized SHD system. By the same token, some models allow for yet another density maximum interior to the orbit of planet c, at ~ 0.05 AU. Such experimental models are characterized by different parameter sets, so a "best-fit model" cannot be determined, unless additional planets are discovered in μ Ara by future observations.

3.2.4. *Remarks on Surface Density Profiles*

A surface density profile of the form $\Sigma(R) \propto R^{-1.5}$ is applicable outside the central core region of the protoplanetary disk of 55 Cnc and the solar nebula (Table 4). The presence of a roughly uniform core is strongly suggested by both theory and observations (see § 1.2.6), and our models suggest that LLDs and SHDs can be distinguished by their core sizes (~ 1 AU and ~ 0.05 AU, respectively). On the other hand, we do not know why both of the nebular disks in Table 3 show the $R^{-1.5}$ trend, although this fact—that we independently obtained the same result (as opposed to two different power laws) from two different planetary systems—argues in favor of our modeling assumptions.

At this point, we do not have any more evidence of the ubiquity of the $R^{-1.5}$ profile among LLDs and SHDs, but we can certainly argue that this density power law is more relevant to planet formation than the profiles from steady-state viscous and irradiated accretion disks (Kitamura et al. [2002], Andrews & Williams [2007], Garaud & Lin [2007], and references therein). The isothermal phase of protostellar collapse that our models address is an extended intermediate phase of the whole process during which the magnetic fields have diffused away, the central core mass is a minute fraction of the solar mass, matter continues being deposited onto the disk from above and below, most of the gas in the disk is molecular, and all the energy produced is efficiently radiated away (see Tohline [2002] for a recent review). At this stage, the evolution of the gas is not driven by viscosity or by ionization because the gas is transparent to radiation; the gas responds fully to the effects of self-gravity and (non-Keplerian) rotation, and this is why it is very encouraging to know that our modeled disks are dynamically stable (§ 2.6). Theoretical calculations of viscous, magnetized, or irradiated accretion disks are not applicable in this regime of protostellar collapse, while observations of thermal radiation from T Tauri stars probe the disks long after the isothermal phase is over, the gas has become opaque to its own radiation, and the grown protostars have imposed nearly Keplerian rotation profiles onto the disks. Therefore, there is no reason to expect that the surface density profiles should have power-law indices of $k = -1$ or softer (seen in T Tauri disks; Kitamura et al. 2002; Andrews & Williams 2007) during the isothermal phase of collapse; and if the planetary results of Kuchner (2004) give any indication about extrasolar systems, we should expect instead k -indices between -1.5 and -2 .

REFERENCES

- Adams, F. C., Laughlin, G., & Bloch, A. M. 2008, *ApJ*, 683, 1117
- Alibert, Y., Baraffe, I., Benz, W., et al. 2006, *A&A*, 455, L25
- Alibert, Y., Mordasini, C., & Benz, W. 2004, *A&A*, 417, L25
- Alibert, Y., Mordasini, C., Benz, W., & Winisdoerffer, C. 2005a, *A&A*, 434, 343
- Alibert, Y., Mousis, O., Mordasini, C., & Benz, W. 2005b, *ApJ*, 626, L57
- Andrews, S. M., & Williams, J. P. 2007, *ApJ*, 659, 705
- Armitage, P. J. 2003, *ApJ*, 582, L47
- Armitage, P. J., Livio, M., Lubow, S. H., & Pringle, J. E. 2002, *MNRAS*, 334, 248
- Barnes, R., Goździewski, K., & Raymond, S. N. 2008, *ApJ*, 680, L57
- Barnes, R., & Quinn, T. 2004, *ApJ*, 611, 494
- Barnes, R., & Raymond, S. N. 2004, *ApJ*, 617, 569
- Bean, J. L., McArthur, B. E., Benedict, G. F. & Armstrong, A. 2008, *ApJ*, 672, 1202
- Bodenheimer, P., Hubickyj, O., & Lissauer, J. J. 2000, *Icarus*, 143, 2
- Bodenheimer, P., & Pollack, J. P. 1986, *Icarus*, 67, 391
- Bryden, G., Beichman, C. A., Trilling, D. E., et al. 2006, *ApJ*, 636, 1098
- Butler, R. P., Marcy, G. W., Williams, E., Hauser, H., & Shirts, P. 1997, *ApJ*, 474, L115
- Butler, R. P., Wright, J. T., Marcy, G. W., et al. 2006, *ApJ*, 646, 505
- Christodoulou, D. M., & Kazanas, D. 2008, *ApJ*, submitted (astro-ph/0706.3205) (CK)
- Christodoulou, D. M., Shlosman, I., & Tohline, J. E. 1995, *ApJ*, 443, 551
- Davis, S. S. 2005, *ApJ*, 627, L153
- Desort, M., Lagrange, A.-M., Galland, F., et al. 2008, *A&A*, preprint (astro-ph/0809.3862)
- Eggenberger, A., Udry, S., & Mayor, M. 2004, *A&A*, 417, 353
- Fischer, D. A., Marcy, G. W., Butler, R. P., et al. 2008, *ApJ*, 675, 790

- Garaud, P., & Lin, D. N. C. 2007, *ApJ*, 654, 606
- Gayon, J., Marzari, F., & Scholl, H. 2008, *MNRAS*, 389, L1
- Gonzalez, G., & Vanture, A. D. 1998, *A&A*, 339, L29
- Hayashi, C. 1981, *Prog. Theor. Phys. Suppl.*, 70, 35
- Ida, S., & Lin, D. N. C. 2004a, *ApJ*, 604, 388
- Ida, S., & Lin, D. N. C. 2004b, *ApJ*, 616, 567
- Ida, S., & Lin, D. N. C. 2005, *ApJ*, 626, 1045
- Jayawardhana, R., Holland, W. S., Kalas, P., et al. 2002, *ApJ*, 570, L93
- Kitamura, Y., Momose, M., Yokogawa, S., et al. 2002, *ApJ*, 581, 357
- Kuchner, M. J. 2004, *ApJ*, 612, 1147
- Laskar, J. 1996, *Celest. Mech. Dyn. Astron.*, 64, 115
- Lecoanet, D., Adams, F. C., & Bloch, A. M. 2008, *ApJ*, preprint (astro-ph/0810.4076)
- Lin, D. N. C., Papaloizou, J. C. B., Terquem, C., Bryden, G., & Ida, S. 2000, *Protostars and Planets IV*, ed. V. Mannings, A. P. Boss, & S. S. Russell (Univ. of Arizona Press: Tucson), 1111
- Lissauer, J. J. 1987, *Icarus*, 69, 249
- Lissauer, J. J. 1993, *ARA&A*, 31, 129
- Lissauer, J. J. 1995, *Icarus*, 114, 217
- Marcy, G. W., Butler, R. P., Fischer, D. A., et al. 2002, *ApJ*, 581, 1375
- Marcy, G., Butler, R. P., Fischer, D., et al. 2005, *Prog. Th. Phys. Suppl.*, 158, 24
- Marcy, G. W., Cochran, W. D., & Mayor, M. 2000, *Protostars and Planets IV*, ed. V. Mannings, A. P. Boss, & S. S. Russell (Univ. of Arizona Press: Tucson), 1285
- McArthur, B. E., Endl, M., Cochran, W. D., et al. 2004, *ApJ*, 614, L81
- Pepe, F., Correia, A. C. M., Mayor, M. 2007, *A&A*, 462, 769
- Pierens, A., & Nelson, R. P. 2008, *A&A*, 482, 333

- Pollack, J. B., Hubickyj, O., Bodenheimer, P., et al. 1996, *Icarus*, 124, 62
- Poveda, A., & Lara, P. 2008, *RMxAA*, 44, 243
- Raghavan, D., Henry, T. J., Mason, B. D., et al. 2006, *ApJ*, 646, 523
- Raymond, S. N., & Barnes, R. 2005, *ApJ*, 619, 549
- Raymond, S. N., Barnes, R., & Gorelick, N. 2008, *MNRAS*, *ApJ*, preprint (astro-ph/0808.3295)
- Raymond, S. N., Barnes, R., & Kaib, N. A. 2006, *ApJ*, 644, 1223
- Santos, N. C., Bouchy, F., Mayor, M., et al. 2004, *A&A*, 426, L19
- Schneider, G. Becklin, E. E., Smith, B. A., et al. 2001, *AJ*, 121, 525
- Tohline, J. E. 2002, *ARA&A*, 40, 349
- Trilling, D. E., Lunine, J. I., & Benz, W. 2002, *A&A*, 394, 241
- Valenti, J. A., & Fischer, D. A. 2005, *ApJS*, 159, 141
- Vogt, S. S., Butler, R. P., Marcy, G. W., et al. 2005, *ApJ*, 632, 638
- Ward, W. R., & Hahn, J. M. 2000, *Protostars and Planets IV*, ed. V. Mannings, A. P. Boss, & S. S. Russell (Univ. of Arizona Press: Tucson), 1135
- Weidenschilling, S. J. 1977, *A&SS*, 51, 153
- Zhou, L.-Y., Ferraz-Mello, S., & Sun, Y.-S. 2008, *Exoplanets: Detection, Formation and Dynamics*, Proc. IAU Symposium No. 249, ed. Y.-S. Sun, S. Ferraz-Mello, & J.-L. Zhou (Cambridge Univ. Press: Cambridge), 119

FIGURE CAPTIONS

Fig. 1.— Analytic density and rotation profiles of the composite equilibrium models described by eqs. (6) and (7) for $x_1 = 100$ and $\delta = 2.1, 2.5,$ and 2.9 . Both profiles are uniform in the core region with $x \leq x_1$.

Fig. 2.— Equilibrium density profile in the midplane of the protoplanetary disk of 55 Cnc. The composite model described in § 2.2 (eq. [6], dashed line) has been adopted for the RHS of the Lane–Emden equation (8) and this differential equation has been integrated numerically subject to the physical boundary conditions (5). The resulting exact solution (solid line) has been fitted to 55 Cnc so that its density maxima (dots) correspond to the observed semimajor axes of the planetary orbits (open circles). Frame (a) shows the radial distance d on a linear scale out to $d = 7$ AU. Frame (b) shows the same radial distance on a logarithmic scale out to $\ln d = 3$ ($d = 20$ AU). The nonrotating analytic solution $\ln \tau(d) = -2 \ln(1 + d^2/8R_0^2)$ from CK (dash-dotted line) is also shown for reference. The numerical solution tracks closely the nonrotating solution near the center, but eventually it has to turn around to approach the (dashed) baseline solution; and this sets off the oscillations in the physical density profile.

Table 4:

THE TWO MODES OF MULTI-PLANET SYSTEM FORMATION

Physical Property	Large Light Disks (Solar System) ^{a,b}	Small Heavy Disks (55 Cancri A) ^{a,c}
Disk		
Metallicity (Z)	Z_{\odot}	$2Z_{\odot}$
Radial Scale (R_0)	0.02 AU	0.001 AU
Radial Size	40–70 AU	6–10 AU
Core Size (R_1)	1 AU	0.05 AU
Core Density (ρ_0)	4×10^{-9}	3×10^{-6}
Rotation		
β_0	0.4	0.1
Rotation Period ($2\pi/\Omega_0$)	12 yr	1 yr
Jeans Period ($2\pi/\Omega_J$)	5 yr	0.1 yr
Gas Surface Density		
Σ_0	2500	75000
$\Sigma(1 \text{ AU})$	2000	1000
$\Sigma(5 \text{ AU})$	200	100
$\Sigma(R \geq R_1) \propto R^k$, $k =$	-1.5	-1.5

NOTES:

(a) cgs units apply unless stated otherwise.

(b) Order-of-magnitude estimates based on the results of CK.

(c) Order-of-magnitude estimates based on the results of this work.

Table 5:

CHARACTERISTICS OF THE OBSERVED PLANETS
AROUND μ ARA (PEPE ET AL. 2007)

Index i	Planet Designation	Orbital Period P_i (days)	Semimajor Axis a_i (AU)	Minimum Mass $M_{min,i}$ (M_J) ^a	Orbital Eccentricity e_i
1	c	9.6386	0.091	0.03321	0.172
2	d	310.55	0.921	0.5219	0.0666
3	b	643.25	1.497	1.676	0.128
4	e	4205.8	5.235	1.814	0.0985

NOTE:

(a) Minimum masses are given in Jupiter masses.

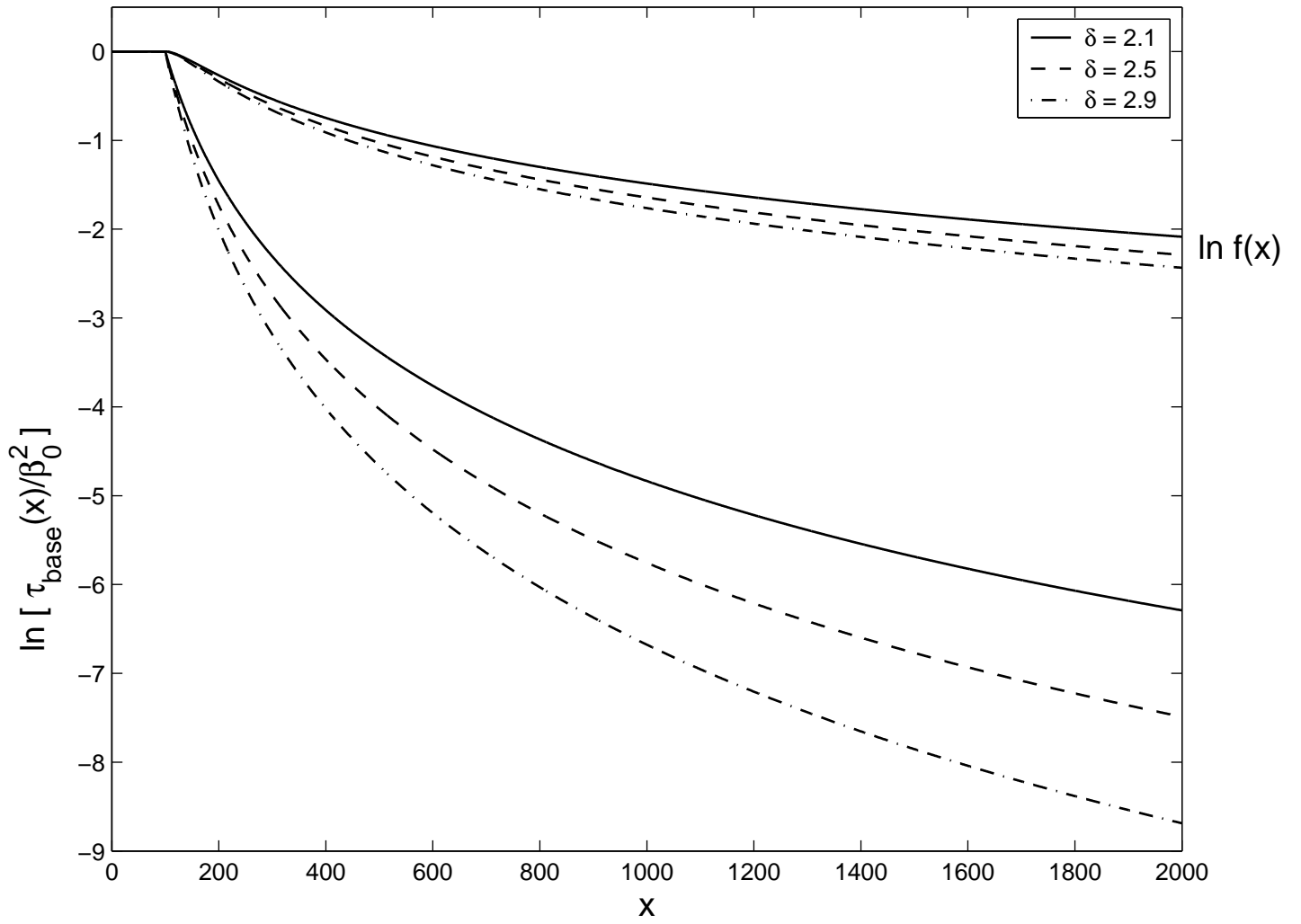


FIGURE 1

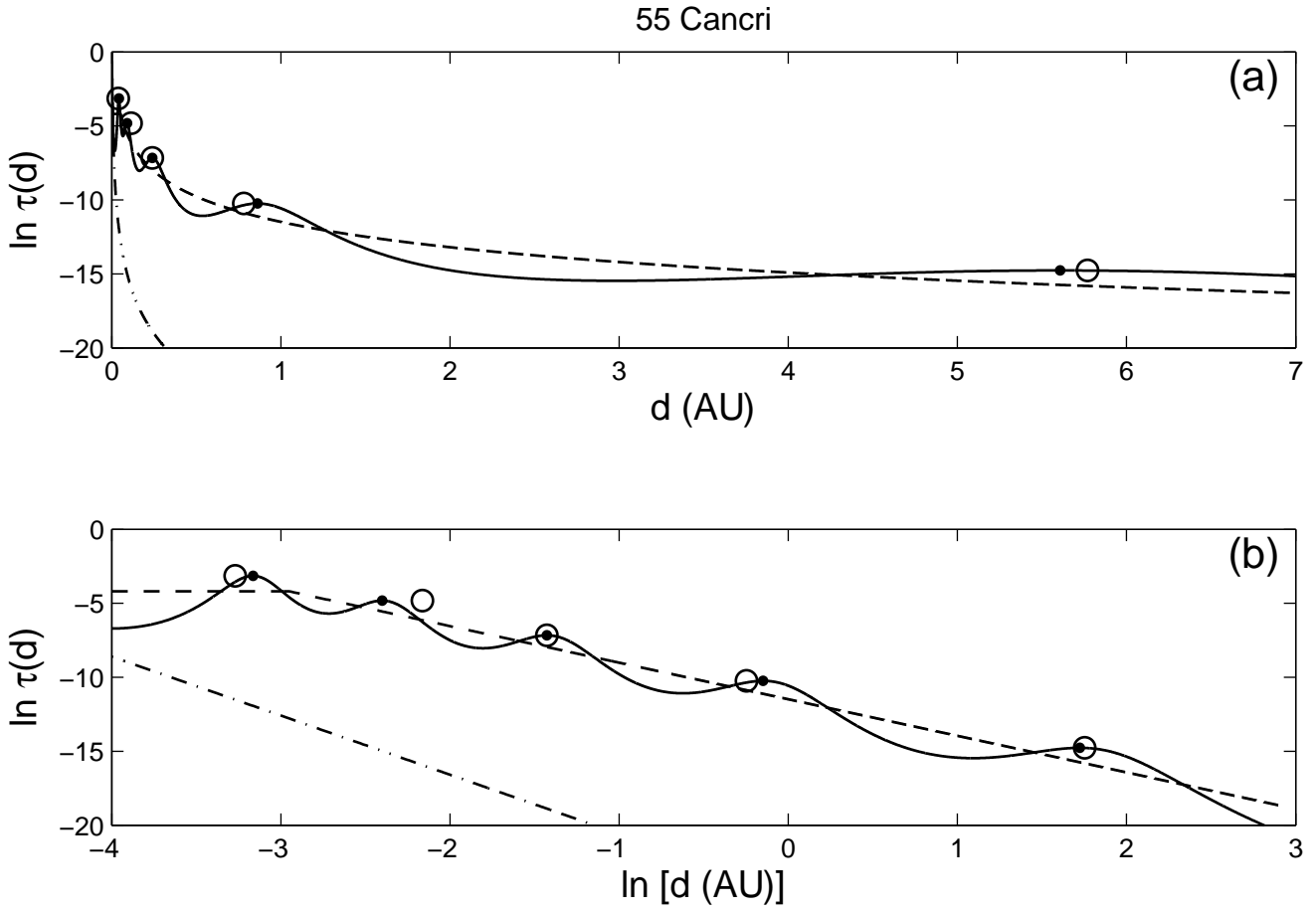


FIGURE 2